1

2

3

4

5

6

7

8

9

10

11

12   **Title:** Voluntary control of illusory contour formation

13

14   **Authors and affiliations:** William J Harrison [1,2,] & Reuben Rideaux [1]

15   [1] Department of Psychology, University of Cambridge

16   Downing Street, Cambridge CB2 3EB, UK

17   [2] Queensland Brain Institute, The University of Queensland

18   QBI Building #79, St Lucia QLD 4072, Australia

19

20   **Corresponding author**: William Harrison (willjharri@gmail.com)

21

22   **Classification:** Biological Sciences; Psychological and Cognitive Sciences

23

24

ABSTRACT

The extent to which visual inference is shaped by attentional goals is unclear. Voluntary attention may simply modulate the priority with which information is accessed by higher cognitive functions involved in perceptual decision making. Alternatively, voluntary attention may influence fundamental visual processes, such as those involved in segmenting an incoming retinal signal into a structured scene of coherent objects, thereby determining perceptual organisation. Here we tested whether the segmentation and integration of visual form can be determined by an observer's goals by exploiting a novel variant of the classical Kanizsa figure. We generated predictions about the influence of attention with a machine classifier, and tested these predictions with a psychophysical response classification technique. Despite seeing the same image on each trial, observers' perception of illusory spatial structure depended on their attentional goals. These attention-contingent illusory contours directly conflicted with equally plausible visual form implied by the geometry of the stimulus, revealing that attentional selection can determine the perceived layout of a fragmented scene. Attentional goals, therefore, not only select pre-computed features or regions of space for prioritised processing, but, under certain conditions, also greatly influence perceptual organisation and thus visual appearance.

SIGNIFICANCE STATEMENT

The extent to which higher cognitive functions can influence perceptual organisation is debated. The role of voluntary spatial attention, the ability to focus on only some parts of a scene, has been particularly controversial among neuroscientists and psychologists who aim to uncover the basic neural computations involved in grouping image features into coherent objects. To address this issue, we repeatedly presented the same novel ambiguous image to observers and changed their attentional goals by having them make fine spatial judgements about only some elements of the image. We found that observers' attentional goals determine the perceived organisation of multiple illusory shapes. We thus reveal that voluntary spatial attention can control the fundamental processes that determine perceptual organisation.

INTRODUCTION

54

55 The clutter inherent to natural visual environments means that goal-relevant objects often

56 partially occlude one another. A critical function of the human visual system is to group

57 common parts of objects while segmenting them from distracting objects and background,

58 a process which requires interpreting an object's borders. Figures which produce illusory

59 contours, such as the classic Kanizsa triangle (Kanizsa, 1976), have provided many insights

60 into this problem by revealing the inferential processes made in determining figure-ground

61 relationships. These figures give rise to a vivid percept of a shape emerging from sparse

62 information, and thus demonstrate the visual system's ability to interpolate structure from

63 fragmented information, to perceive edges in the absence of luminance discontinuities, and

64 to fill-in a shape's surface properties (for a review, see Shapley, Rubin, & Ringach, 2004).

65 In the present study, we exploit these figures to investigate whether voluntary attention

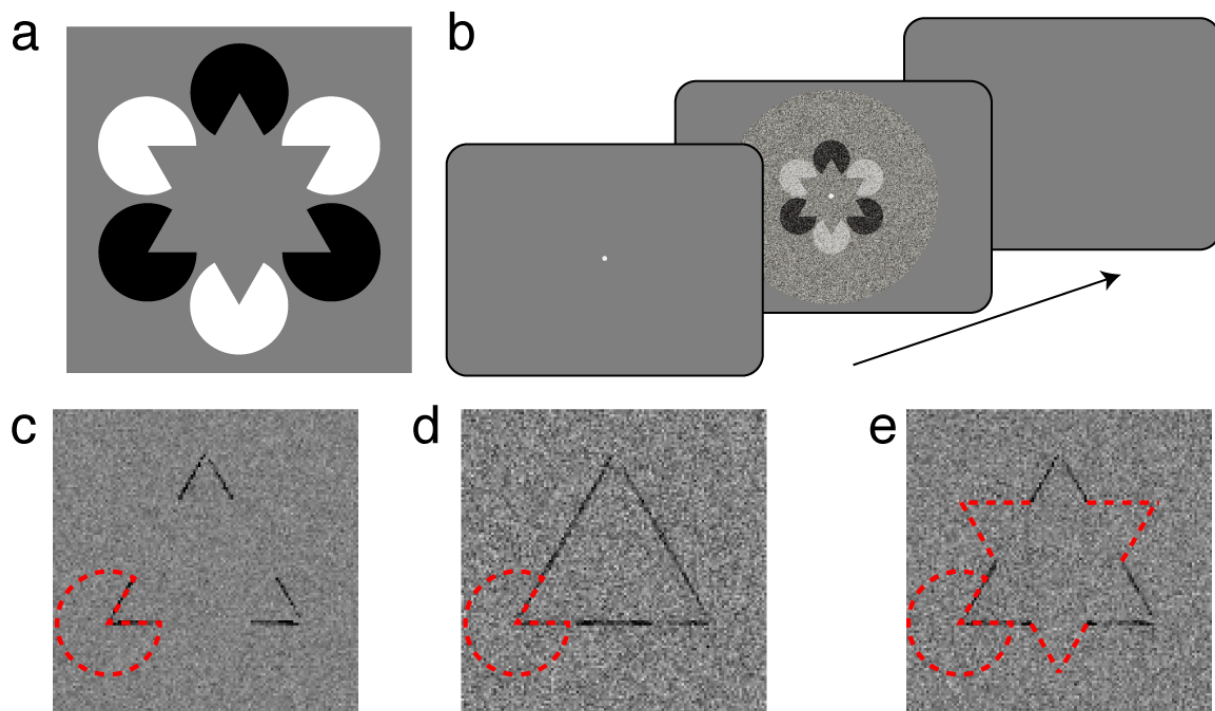66 influences perceptual organisation.

67

68 Most objects can be differentiated from their backgrounds via a luminance-defined border.

69 The visual system is tasked with allocating one side of the border to an occluding object,

70 and the other side to the background. This computation can be performed by neurons in

71 macaque visual area V2 whose receptive fields fall on the edge of an object (Zhou,

72 Friedman, & von der Heydt, 2000). These "border-ownership" cells can distinguish figure

73 from ground even when the monkey attends elsewhere in the display (Qiu, Sugihara, & von

74 der Heydt, 2007), and psychophysical adaptation aftereffects suggest such cells also exist

75 in humans (von der Heydt, Macuda, & Qiu, 2005). Further, neurophysiological work has

76 revealed that V2 cells also process illusory edges (von der Heydt, Peterhans, &

77 Baumgartner, 1984), though it is unclear whether those cells possess the same properties

78 as border-ownership cells. These findings have contributed to the claim that visual structure

79 is computed automatically and relatively early in the visual system, and that visual attention

80 is guided by this pre-computed structure (Mihalas, Dong, von der Heydt, & Niebur, 2011).

81

82 It is also known, however, that visual attention can modulate the perception of figure-ground

83 relationships of luminance-defined stimuli. Both voluntary and involuntary forms of

84 attentional allocation can impact higher level cognition (Posner, 2014) and basic perception

85   (Carrasco, 2011). Allocating visual attention to an area of space, for example, prioritises

86   processing of stimuli presented at that location relative to other locations (Posner, 1980),

87   and can alter apparent contrast (Carrasco, Ling, & Read, 2004). As early as 1832, Necker

88   described his ability to alter the apparent depth of an engraved crystalline form, now referred

89   to as a Necker cube, via an overt shift of attention (Necker, 1832). More recent

90   psychophysical work has shown that voluntary attention can alter perceived depth order

91   (Driver & Baylis, 1996) as in the case of Rubin's face-vase illusion (Rubin, 1915)(Wagemans

92   et al., 2012), surface transparency (Tse, 2005), speed (Anton-Erxleben, Henrich, & Treue,

93   2007; Turatto, Vescovi, & Valsecchi, 2007), contrast (Carrasco et al., 2004; Liu, Abrams, &

94   Carrasco, 2009; Stormer, McDonald, & Hillyard, 2009) and spatial frequency (Abrams,

95   Barbot, & Carrasco, 2010; Gobell & Carrasco, 2005). Furthermore, visual attention has

96   been shown to facilitate visual grouping according to Gestalt rules at both the

97   neurophysiological (Wannig, Stanisor, & Roelfsema, 2011) and behavioural (Barbot, Liu,

98   Kimchi, & Carrasco, 2018; Houtkamp, Spekreijse, & Roelfsema, 2003) level. For instance,

99   (Barbot et al., 2018) found that the apparent perceptual organization of luminance defined

100 multielement arrays is either intensified or attenuated by the presence or absence of covert

101 attention, respectively. These findings raise the possibility that, regardless of whether it is

102 necessary, visual attention may play a determining role in visual appearance under certain

103 conditions. However, because these previous studies involved physically defined stimuli, it

104 remains unclear whether visual attention simply modulates pre-attentively computed

105 structure as suggested by neurophysiological work (McMains & Kastner, 2011; Qiu et al.,

106 2007), or whether structural computations depend on the state of attention. Rivalrous illusory

107 figures are perfectly suited to address this issue: if attending to one illusory figure results in

108 illusory contours that directly conflict with the form of another illusory figure, then structural

109 computations must depend on attention.

110

111 To investigate the influence of voluntary attention on perceptual organisation, here we

112 combined a novel illusory figure with an attentionally demanding task, exploiting human

113 observers' propensity to use illusory edges when making perceptual decisions (Gold,

114 Murray, Bennett, & Sekuler, 2000). We developed a novel Kanizsa figure (**Fig. 1a**), in which

115 "pacman" discs are arranged at the tips of an imaginary star. This figure includes multiple

4

116　Gestalt cues that promote the segmentation and integration of various forms not defined by

117　the physics of the stimulus (Harrison, Ayeni, & Bex, 2019). We predict that, because some

118　of these cues suggest competing configurations, selective attention can bias which figure

119　elements are assigned to figure and which to ground. Although such a hypothesis is

120　relatively uncontroversial, the critical question is whether grouping via selective attention

121　promotes illusory contour formation in direct conflict with competing implied form. For

122　example, while the black inducers of **Figure 1a** form part of an implied star, in isolation the

123　black inducers imply an illusory triangle that competes with both the star form as well as a

124　second illusory triangle implied by the white inducers. The dependence of such perceptual

125　organisation on voluntary attentional selection thus can reveal the extent of top-down

126　processing on visual appearance. We therefore assessed whether the apparent

127　organisation of the figure is determined by which inducers are attended.

128

Figure 1. Novel illusory figure and design used to test the influence of attention on perceptual organisation. a) Our variant of the classic Kanizsa figure. "Pacman" inducers are arranged such that a star appears to occlude black and white discs. Whereas the ensemble of features may produce the appearance of a star, grouping features by polarity leads to competing illusory triangles. We test whether attending to one set of inducers (e.g. the white inducers) leads to interpolation of the illusory edge. b) Example trial sequence. After an observer fixates a spot, the illusory figure with overlaid Gaussian noise is displayed for 250ms. The observer's task was to report whether the tips of the upright or inverted triangle were narrower or wider than an equilateral triangle. The target triangle was cued prior to, and held constant throughout, each testing block. The observer's perceptual reports were then correlated with the noise on each trial to produce classification images. (c - e) Support vector machine (SVM) classifier images. We had a SVM classifier perform "narrow" vs "wide" triangle judgements after training it on three different protocols: (c) inducers, a (d) triangle, or a (e) star (see Methods). Dashed red lines show the location of a pacman for reference, and in (e) the tips of the star that do not influence classification.

RESULTS

We used a response classification technique that allowed us to simultaneously assess where observers' attention was allocated, and whether such attentional allocation resulted in visual interpolation of illusory edges. At the beginning of each block of testing, observers were cued to report the relative jaw size of the inducers forming an upright (or inverted) triangle, corresponding to the white (or black) elements in **Figure 1a**. By adding random visual noise to the target image on each trial (**Fig. 1b**), we could use reverse correlation to

6

151   measure "classification images". An observer's classification image quantifies a correlation

152   between each pixel in the image and the perceptual report revealing which spatial locations

153   are used for perceptual decisions (Abbey, Eckstein, & Bochud, 1999; A. J. . J. Ahumada,

154   Beard, & Ellis, 1997; A. J. Ahumada, 1996; A. Ahumada & Lovell, 1971; Beard & Ahumada,

155   Jr., 1998; Gold et al., 2000).

156

157   We generated hypotheses regarding how observers' voluntary attention may influence their

158   perception of this figure. We used a support vector machine (SVM) classifier to judge small

159   changes to a triangle image after training it on one of three different protocols (**Supp. Fig.**

160   **1**). First, we generated a prediction of the hypothesis that observers can attend to the correct

161   inducers, but do not perceive illusory edges, by training a model to discriminate only the

162   jaws of the inducers. This model is analogous to that of an ideal observer and reveals that

163   only structure at the edges of the stimuli are used in generating a response (**Fig. 1c**). We

164   next generated predictions of how illusory edges could be interpolated in this task. In one

165   case, we assumed illusory contours would be formed between attended inducers. We thus

166   trained the classifier to discriminate whether a triangle's edges were bent outward or inward,

167   and found a classification image approximating a triangle (**Fig. 1d**). In the other case, we

168   assumed that, although selective attention may guide the correct perceptual decision, the

169   illusory form of a star may be determined pre-attentively according to the physical structure

170   of the entire stimulus. In this case, we trained the classifier to discriminate whether

171   alternating tips of a star, i.e., the tips corresponding to a set of cued inducers, were relatively

172   wide or narrow. The resulting classification image reveals edges that are interpolated

173   beyond the inducers, but that they do not extend beyond the alternating star tips (**Fig. 1e**).

174   These predictions not only provide qualitative comparisons for our empirical data, but they

175   also allow us to formally test which training regime produces a classification image that most

176   closely resembles human data.

177

178   To motivate observers to attend to only one possible configuration of the illusory figure, they

179   were cued to report the relative jaw size ("narrow" or "wide") of only a subset of pacmen

180   positioned at the tips of an imaginary star (**Fig. 1a**). Each cued triangle was defined by three

181   inducers, the jaw-sizes of which were varied from 60° (an implied equilateral triangle)

7

according to an adaptive staircase (see Materials and Methods). In an early investigation into illusory contour perception, Ringach and Shapley (1996) found that observers' perceptual thresholds were less than an angular degree with similarly sized stimuli. Specifically, observers were instructed to report only the jaw size of inducers forming an upward (or downward) triangle within a testing block. The non-cued inducer jaws varied independently of the cued inducers and thus added no information regarding the correct response. To derive the spatial structure used for perceptual decisions, we added Gaussian noise to each trial and classified each noise image according to the observers' responses (**Fig. 1b**). To create the classification image for each observer, we summed all noise images for narrow reports and subtracted the sum of all noise images for wide reports (see Methods). We collapsed across inducer polarity by inverting the noise on trials in which the white inducers were cued, and across cue direction by flipping the noise on trials in which the downward facing illusory triangle was cued. The resulting images quantify the correlation between each stimulus pixel and the observer's report. In order to analyse a single axis of emergent spatial structure, we first averaged each observer's data with itself after rotating 120° and 240° such that correlations were averaged over the three sides of the triangle. Although this step involved bilinear interpolation of neighbouring pixels, no other averaging or smoothing was performed, and this averaging is therefore most likely to only reduce the strength of emergent illusory structure.

Classification images for three observers and their mean are shown in **Figure 2a** (see **Supp. Fig. 2a** for unrotated classification images). Images are normalised to the "attend upright black inducers" condition; black pixels indicate locations where dark and light noise was correlated with narrow and wide judgements, respectively, and white pixels indicate the opposite relationship. There are two obvious patterns that emerge. First, it is clear that observers based their reports on pixels within the jaws of the cued inducers, indicating that only some regions of the image – those aligned with the attended inducers – influenced perceptual decisions. Note the difference in the sign of the correlation between the edges and tips of the triangle – noise pixels in these regions have the opposite influence on narrow/wide decisions, which is likely due to an illusory widening of the jaw centre which is not registered by the SVM (cf. **Fig. 1d**). Second, the edges clearly extend beyond the red

8

213   inducer outline shown in the mean image, revealing observers' reports were influenced by

214   illusory contours. However, it is also apparent that the spatial structure is non-uniform, with

215   weaker correlations in the centre of the illusory edges than in the corners of the inducers.

216   We therefore quantitatively test the extent of illusory contour formation below.

217

218   To test whether the illusory edge interpolation extended into the region of the implied

219   competing figure, we performed two analyses. First, we used Bayesian and Students' one-

220   sampled t-tests to assess the pixel values along the edge of the triangle implied by the

221   attended inducers (see red line in **Fig. 2a**). We selected only pixels that fell within the bounds

222   of the competing implied triangle (see Methods and grey shaded regions of **Fig. 2b**), and

223   found that these 18 pixels were below zero for the naïve participant (mean and sem: $-3 \pm .9$

224    $\times 10^{-3}$, $BF_{10}=18.365$, $t(17)=3.585$, $p=0.002$, $d = 0.845$), observer A2 (mean and sem: $-5 \pm .7$

225    $\times 10^{-3}$, $BF_{10}=8,141.356$, $t(17)=6.944$, $p<0.001$, $d = 1.637$), and the group (mean and sem: -

226    $3 \pm .4 \times 10^{-3}$, $BF_{10}=16,580$, $t(17) = 7.38$, $p<0.001$, $d = 1.738$), but not for A1 (mean and sem:

227    $-1 \pm 1 \times 10^{-3}$, $BF_{10}=0.431$, $t(17)=1.15$, $p=0.266$, $d = 0.204$). The lack of a difference in

228   observer A1 may be due to a difference in task related strategy and or increased lapse rate.

229
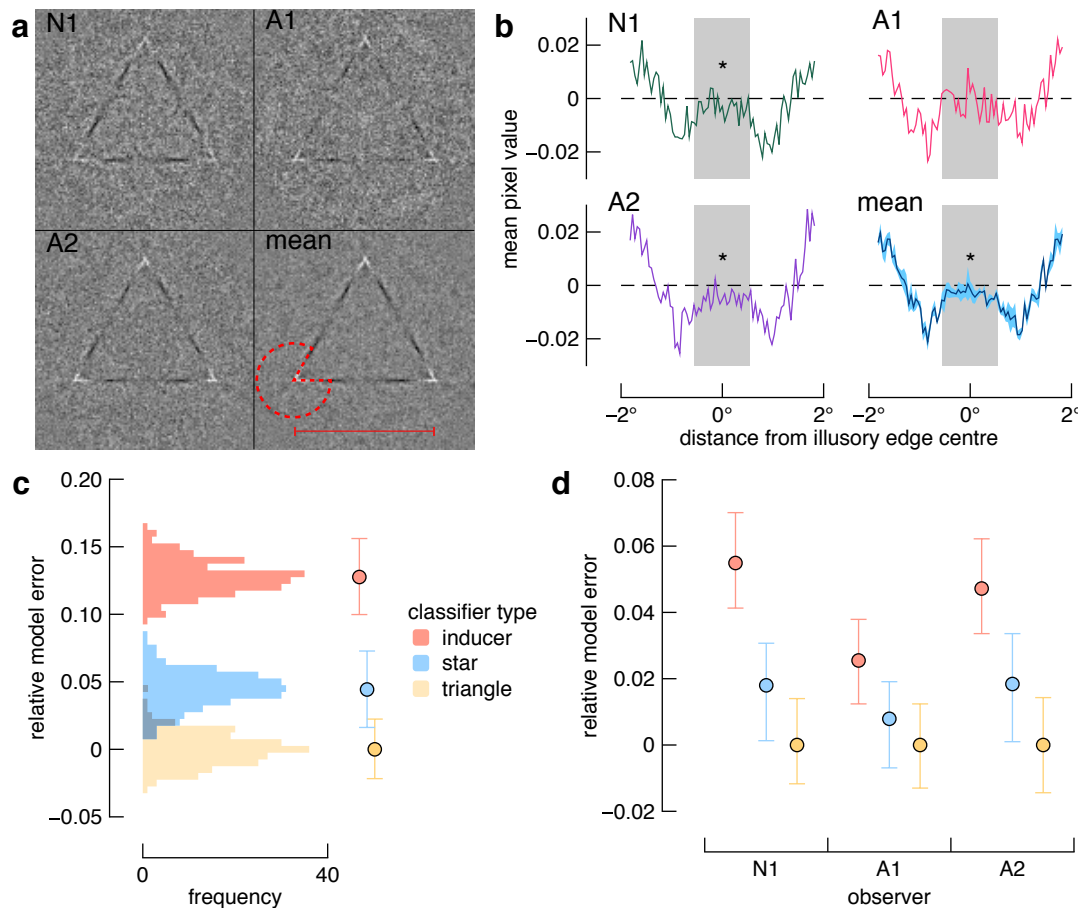
Figure 2. Classification image results. a) The individual and average classification images, normalized to the "attend upright black inducers" condition. Black pixels indicate locations where dark and light noise was correlated with narrow and wide judgements, respectively, and white pixels indicate the opposite relationship, after 9984 trials per participant. Data have not been smoothed, but were first averaged across triangle edges and cropped to be 122x122 pixels. In the mean image, a pacman outline is shown for reference, and a red line indicates the spatial range of the implied triangle edge (from which data in (b) are shown). b) Pixel values along the illusory edge. The grey shaded region corresponds to a conservative estimate of the extent of a gap in the edge that would appear if observers necessarily saw a star shape (e.g. Fig. 1e). The blue shaded region in the mean plot shows ±one standard error; asterisks indicate differences from zero ($BF_{10} > 10$ and $p < 0.05$; see text). N1 is the naïve participant; A1 and A2 are authors. c) Comparison of SVM models for averaged data. Distributions show comparisons of the mean classification image to the output of each SVM prediction, repeated 200 times. Data points and error bars represent the mean and 95% confidence intervals, respectively, for each SVM training regime. Model error has been normalised relative to the model with the least error, which is the model in which the SVM is trained to perceive a triangle within the attended inducers. d) Comparison of SVM models for each observer. Colours are as per panel (c).

We next quantified the spatial structure content of the classification image by testing which prediction generated by the SVM was most similar to the human data (see **Fig. 1c-e**). For

10

249 each model, we generated 200 predictions, each with a unique distribution of noise, and

250 computed the sum of squared errors between predictions and the mean classification image

251 produced by the human observers (see Materials and Methods). The resulting distributions

252 of error, normalised to the best model, are shown in **Figure 2c**, and reveal that the model in

253 which we trained the classifier to perceive a complete triangle is the best fit to the data (z-

254 test comparing the mean error for the triangle SVM versus the distribution of error for the

255 star or inducer SVM: p's < 0.0001). The pattern of results was the same for all observers

256 (**Fig. 2d**): for the inducer, star, and triangle templates, respectively, the mean standardised

257 model errors (±one standard deviation) were N1: 0.055 (0.007), 0.018 (0.008), 0 (0.007);

258 A1: 0.026 (0.006), 0.008 (0.006), 0 (0.007); A2: 0.047 (0.008), 0.018 (0.008), 0 (0.007). Z-

259 tests comparing the mean error for the triangle SVM versus the distribution of error for the

260 star or inducer SVM were all significant (all p's < 0.0001). Taken together, these analyses

261 reveal illusory contour formation between attended visual elements, and this interpolation

262 occurred despite the contour conflicting with equally plausible implied spatial structure.

263

264 We next tested the spatial specificity of illusory contour formation. In the preceding analyses

265 presented in Figure 2b, we selectively tested only a single row of pixels aligned with the

266 mouths of the inducers. For the two participants who showed a clear effect, we next tested

267 how spatially specific visual interpolation was by repeating the same analysis but for the row

268 of pixels above and below the triangle boundary implied by the geometry of the attended

269 inducers. Quite surprisingly, we found good evidence that there was an absence of illusory

270 contour formation for the pixels below the implied triangle boundary (N1: BF_{01} = 3.19; A2:

271 BF_{01} = 3.31), and equivocal evidence for the pixels above the implied triangle boundary (N1:

272 BF_{10} = 1.05; A2: BF_{01} = 1.83). We therefore found evidence that only a single row of pixels

273 extending between the inducer edges contributed to observers' perceptual decisions. These

274 results thus reveal that the strength of illusory contours was highly precisely aligned to the

275 geometry of the triangle implied by the attended inducers. Consistent with this observation,

276 psychophysical thresholds for identifying the relative inducer jaw size were reliably highly

277 precise across testing sessions (see **Supp. Fig. 2b**). Across sessions, the mean thresholds

278 (±one standard error) for observer N1, A1, and A2, were 0.86° ± .03°, 0.84° ± .02°, and 0.66°

279 ± .03°.

280

281   Our data further address the extent to which the non-cued figural elements may have

282 influenced perceptual judgements. In our experiment, the non-cued inducer jaw size was

283 independent of the cued inducer jaw size, and was thus uninformative of the correct report.

284 Indeed, we found no evidence in the classification image that observers' perceptual

285 decisions were guided by these task-irrelevant cues. We modelled the possibility that these

286 non-cued elements were nonetheless grouped to form a star. In such a case where a star

287 was perceived, the task could still be performed accurately were observers to base their

288 reports on only the edges shared by the star and the triangle implied by the cued inducers.

289 As expected, the SVM prediction of pre-attentive figure-ground segmentation shows gaps

290 in the sides of the classification image triangle (**Fig 1e**). Note that this model is equivalent

291 to observers having perceived a whole star, but with a later stage attentional signal focussed

292 on only some regions of the pre-computed figure. Because we designed our illusory figure

293 to be geometrically invertible, the extent of the illusory star form is pronounced if we sum

294 the model's classification image with a flipped version of itself (**Fig. 3a**). In **Figure 3b**, we

295 show the result of performing this step with the observers' average classification image.

296 Very similar patterns of results were found for all individual images (**Supp. Fig. 3**).

297

298 Although flipping the classification image and producing a star-like figure may be somewhat

299 trivial, more important is how the edges of the star are formed. We wish to test whether the

300 extent of the illusory lines matches what would be expected were observers to have relied

301 on a pre-attentively computed star form, rather than two superimposed triangles determined

302 by attentional selection. The critical aspect of the star-like figure shown in Figure 3b is

303 therefore whether or not the lines that form the star have terminators at the point where they

304 intersect (ie. the inner corners of the implied star). This is the case in Figure 3a because we

305 are using the star model to generate the classification image. For observers' data in Figure

306 3b, on first glance the same appears to be the case: the emergent features appear to stop

307 precisely at the point of intersection, suggesting observers perceived a star but based their

308 reports on only some parts of this figure. These qualitative results, however, are in contrast

309 to the SVM analysis, presented above (Fig. 2), in which we found that correlated noise in

310 observers' classification images is best explained by observers having attended to the cued

311   triangle. Thus, a remaining critical question, which we address below, is whether we can

312   quantify the proportion of trials in which observers relied on different forms implied by the

313   inducers.

314
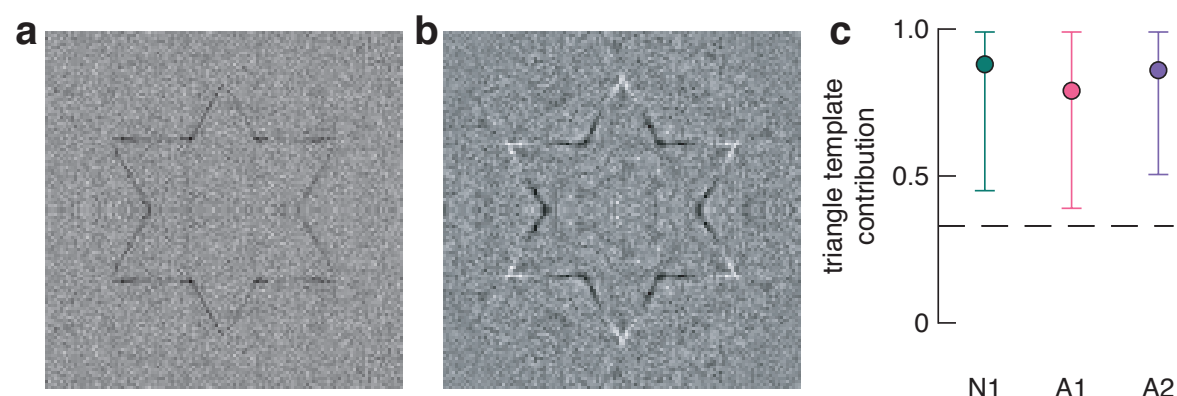
315   **Figure 3**. Pre-attentive grouping. a) Geometric form prediction of unattended grouping. The classification

316   image derived from our SVM was summed with a flipped version of itself. Note that the inner corners of the

317   star are well aligned due to the design of our original Kanizsa figure. b) Geometric form in observers' data.

318   The mean classification image was summed with a flipped version of itself, and reveals the strength of illusory

319   edges are well aligned to the implied star. c) Results of mixture modelling used to explore the correspondence

320   between fluctuations of illusory edge strength and implied figure geometry. The best fitting model for each

321   observer was one in which attention determined perceptual outcome in 84% of trials. The dashed line indicates

322   the proportion expected from a purely stochastic process. Error bars show 95% confidence intervals.

323

324   In contrast to our initial quantitative analyses, the results of which suggest visual attention

325   determines which of two illusory triangles were perceived on a trial (**Fig. 2**), qualitative

326   inspection of the star-like form shown in Figure 3b suggests observers may have based their

327   reports on only some parts of a pre-attentively computed star. However, there are at least

328   three possible explanations for the near-perfect alignment of changes in illusory edge

329   strength with the implied star figure (**Fig. 3b**). First, as discussed, a similar classification

330   image would have been obtained had observers perceived a star on every trial, a possibility

331   which we discounted by our quantitative analysis of the illusory edge, described above (Fig.

332   2). Second, this qualitative result could be generated if trial-by-trial perceptual organisation

333   was stochastic, such that observers perceived each possible configuration approximately

334   equally often across trials. Under this hypothesis, the resulting illusory contours shown in

335   **Figure 2a** are incidental rather than being determined by observers' attentional goals. The

336   third possible explanation is that observers' voluntary allocation of attention determined the

337 outcome on most, but not all, trials. To distinguish between the two latter possibilities, we
338 used mixture modelling to quantify the proportion of trials in which observers' percept
339 depended on attentional instructions (see Materials and Methods). A purely stochastic
340 process would be implied were the proportion of trials accounted for by the triangle template
341 no different from 0.33 (i.e. the apparent top-most surface was equally often a star, the cued
342 triangle, or the non-cued triangle, see **Fig. 1c-e**). However, in the best fitting model, the
343 attention-contingent triangle template contributed to 84% of trials on average, which is much
344 greater than expected by a stochastic process (**Fig. 3c**). At the individual level, the triangle
345 contributions (and 95% confidence intervals) for N1, A1, and A2 were 88% (45% - 100%),
346 79% (39% - 99.5%), and 86% (50.5% - 100%), respectively. This mixture modelling is thus
347 consistent with observers' attentional goals determining illusory contour interpolation on the
348 vast majority of trials.

349

350 **DISCUSSION**

351 We used classification images to address whether voluntary attention determines a scene's
352 apparent visual structure. Using a psychophysical response classification paradigm we
353 tested which of three competing model predictions best describes the influence of attention
354 on illusory contour formation. Our results clearly show that voluntary attention can guide
355 the fundamental processes involved in perceptual organisation of illusory structure.

356

357 Unlike previous studies that show visual attention modulates the appearance of physically
358 defined surfaces (e.g., attending to different surfaces of the Necker cube (Necker, 1832)),
359 our study shows a rich interaction between attention and endogenously generated percepts.
360 Classification images reveal the spatial location of noise elements that influence observers'
361 responses, whereas interpreting subjective phenomenology is more difficult. However, our
362 stimulus design ensured that the classification images reveal information about the
363 perceived depth order of image elements. The presence of lines in the classification image
364 that extend between the inducers is clear evidence that at least two of three observers based
365 their judgements on the perception of a figure whose edges occlude the competing (non-
366 cued) shape information. Given that the illusory edges of the triangle implied by the attended
367 inducers directly conflict with the regions of the competing implied figures (i.e., the star and

14

368 inverted triangle), our finding that illusory edges were interpolated between attended

369 inducers reveals that attention can determine depth order, even when figures and ground

370 are illusory. Spatial structure is thus computed by neural operations that are at least partially

371 contingent on the voluntary state of the observer. The precision of illusory contours was

372 nonetheless tightly aligned to the geometry of luminance defined structure, indicating these

373 inferential processes are also highly contingent on scene or task context. Indeed, observers'

374 psychophysical thresholds for the inducer task reveal a correspondence between their

375 precise objective psychophysical performance and subjective classification image.

376

377 We found clear inter-participant differences in the classification images. First, we found a

378 clear effect of edge completion in our initial analysis of edge completion in only two out of

379 three observers (Fig. 2). Such a difference across participants is not exceptional: Gold and

380 Shubel (2006) also found classification image evidence of illusory edges in two out of three

381 participants. Nonetheless, although the effect did not reach significance for one observer in

382 our data, the same general direction of results was found in both the classification image

383 analysis (Fig. 2b) and the same results were found in the individual SVM model comparisons

384 (Fig. 2d). A degree of homogeneity of our results across participants is also reflected by the

385 fact that the group-average effect was significant. Importantly, the critical effect of a fully

386 interpolated illusory edge was found in the naïve observer's data, and, across participants,

387 we found relatively strong effect sizes of d = 0.845 (N1), d = 1.637 (A2), and d = 0.204 (A1)

388 despite not being significant for A1. The second inter-participant differences we found were

389 in the raw classification images that reveal varying degrees of completeness (Supp. Fig. 2).

390 For the two observers where the effect was significant, at least two edges of the triangle are

391 clearly visible, and for the remaining observer one edge is clearly visible. We can think of at

392 least three possible explanations for these individual differences (similar between-observer

393 differences were reported by Gold et al, 2000, and Gold & Shubel, 2006). First, observers

394 may have interpolated the edge of a single or pair of unconnected lines between the cued

395 inducers. Second, observers perceived a triangle, but only used part of this triangle to

396 perform the task. Third, there are individual biases in attentional allocation that differentially

397 influenced interpolation of the different edges. Given the strength of the Kanizsa illusion,

398 i.e., the perception of a triangle, we think that the latter two explanations are more likely,

15

399 however we cannot definitively show this with the current data. The conclusion that attention

400 influences illusory contour formation is equally valid under either of these explanations.

401

402 We were able to quantify the influence of non-cued stimuli on perception by measuring a

403 classification image across the entire stimulus. We found that changes in the strength of

404 illusory contour formation between attended inducers were aligned with form implied by the

405 non-cued inducers. Our mixture modelling suggests that the non-cued stimuli influenced

406 performance on approximately 16% of trials. Such a contribution of task-irrelevant features

407 on perceptual decisions could be attributed to lapses in attentional allocation, or variability

408 in the feed-forward processing of the incoming signal. Measuring perceived form in the

409 absence of visual attention is notoriously difficult (Wagemans et al., 2012), which is perhaps

410 one reason why many studies of figure-ground organisation rely on single-unit recordings.

411 Whereas neurophysiological recordings have revealed the brain regions involved in

412 perceptual organisation, they have left open the question of perceptual phenomena. Our

413 data show that the influence of attention on perception is constrained by task-irrelevant

414 information, providing yet further evidence that visual experience is the combination of both

415 bottom-up and top-down processes. This conclusion sheds light on previous work in which

416 competing colour adaptation after-effects are biased according to alternating illusory

417 contours at a similar location (van Lier, Vergeer, & Anstis, 2009). In these demonstrations,

418 the onset of inducer elements likely attracts an observer's attention, resulting in perceptual

419 completion processes specific to only the implied shape of attended elements. Surface

420 filling-in would then follow the contours of the implied form (Poort et al., 2012). Indeed, other

421 recent research from our lab reveals similar interactions may occur between attention and

422 surface filling-in (Harrison et al., 2019).

423

424 The influence of attention on figure-ground segmentation may be explained by feedback

425 signals from the lateral occipital complex (Murray et al., 2002; Stanley & Rubin, 2003) that

426 could act as early as V1 (Wannig et al., 2011), but also may involve modulating responses

427 of border-ownership cells in V2 (Qiu et al., 2007). Border-ownership cells indicate which side

428 of a border is an object versus ground. Previous work showing the activity of border-

429 ownership cells is modulated by visual attention (Qiu et al., 2007) has been limited to

16

430 luminance-defined borders. Our finding that information inferred by the visual system is
431 influenced by voluntary attention suggests that attentional modulation of border-ownership
432 may similarly apply to illusory contours (R von der Heydt et al., 1984). Early psychophysical
433 work suggested that illusory contours are perceived in the absence of attention (Davis &
434 Driver, 1994; Mattingley, Davis, & Driver, 1997), but did not address the question of whether
435 illusory contours can be formed *because* of voluntary attention, which we have shown here.
436 Our findings are also distinct from other recent work that found attention can influence the
437 appearance of existing surfaces (Tse, 2005). In our study, visual attention had a causal role
438 in forming the structure from which perceptual decisions were made. We anticipate that our
439 simple stimulus and task design may prove to be a useful neurophysiological assay to test
440 further the neural substrates governing the interaction between voluntary attention and
441 perceptual organisation.

442

443 **MATERIALS AND METHODS**

444 **Observers**. Three healthy subjects, one naïve (N1) and two authors (A1 & A2 corresponding
445 to authors RR and WH, respectively), gave their informed written consent to participate in
446 the project, which was approved by the University of Cambridge Psychology Research
447 Ethics Committee. All procedures were in accordance with approved guidelines. Simulations
448 were run to determine an appropriate number of trials per participant to ensure sufficient
449 statistical power, and our total sample is similar to those generally employed for
450 classification images. All participants had normal vision.

451

452 **Apparatus**. Stimuli were generated in MATLAB (The MathWorks, Inc., Matick, MA) using
453 Psychophysics Toolbox extensions (Brainard, 1997; Cornelissen, Peters, & Palmer, 2002;
454 Pelli, 1997). Stimuli were presented on a calibrated ASUS LCD monitor (120Hz,
455 1920×1200). The viewing distance was 57 cm and participants' head position was stabilized
456 using a head and chin rest (43 pixels per degree of visual angle). Eye movement was
457 recorded at 500Hz using an EyeLink 1000 (SR Research Ltd., Ontario, Canada).

458

459 **Stimuli and task**. The stimulus was a modified version of the classic Kanisza triangle. Six
460 pacman discs (radius = 1°) were arranged at the tips of an imaginary star centred on a

461   fixation spot. The six tips of the star were equally spaced, and the distance from the centre

462   of the star to the centre of each pacman was 2.1°. The fixation spot was a white circle (0.1°

463   diameter) and a black cross hair (stroke width = 1 pixel). The stimulus was presented on a

464   grey background (77.5 cd/m^2). The polarity of the inducers with respect to the background

465   alternated across star tips. For half the trials, the three inducers forming an upright triangle

466   were white, while the others were black, and for half the trials this was reversed. Inducers

467   had a Weber contrast of .75.

468

469   We added Gaussian noise to the stimulus on each trial to measure classification images.

470   Noise was 250 x 250 independently drawn luminance values with a mean of 0 and standard

471   deviation of 1. Each noise image was scaled without interpolation to occupy 500 x 500

472   pixels, such that each randomly drawn luminance value occupied 2 x 2 pixels (.05° x .05°).

473   The amplitude of these luminance values was then scaled to have an effective contrast of

474   0.125 on the display background, and were then added to the Kanizsa figure. Finally, a

475   circular aperture was applied to the noise to ensure the edges of the inducers were equally

476   spaced from the noise edge (**Fig. 1b**).

477

478   The jaw size of inducers was manipulated such that they were wider or narrower than an

479   equilateral triangle, which would have exactly 60° of jaw angle for all inducers. The

480   observer's task was to indicate whether the jaws of the attended inducers was consistent

481   with a triangle that was narrower or wider than an equilateral triangle. Prior to the first trial

482   of a block, a message on the screen indicated which set of inducers framed the "target"

483   triangle, and this was held constant within a block but alternated across blocks. The polarity

484   of the target inducers and whether the triangles were narrow or wide was pseudorandomly

485   assigned across trials such that an equal number of all trial types were included in each

486   block. The relative jaw size of attended inducers was independent of the unattended

487   inducers; thus, the identity of the non-target triangle was uncorrelated with the correct

488   response.

489

490   Each trial began with the onset of the fixation spot and a check of fixation compliance for

491   250 ms. Following an additional random interval (0-500 ms uniformly distributed), the

492   stimulus was presented for 250 ms, after which only the background was presented while

493   observers were given unlimited duration to report the jaw size using a button press. The

494   next trial would immediately follow a response. Throughout the experiment, eye tracking

495   was used to ensure observers did not break fixation during stimulus presentation. If gaze

496   position strayed from fixation by more than 2° the trial was aborted and a message was

497   presented instructing them to maintain fixation during stimulus presentation, and then the

498   trial was repeated. Such breaks in fixation were extremely rare for all participants.

499

500   A three-down one-up staircase procedure was used to progress the difficulty of the task by

501   varying the difference of the jaw size from 60° (i.e., from what would form an equilateral

502   triangle). On each trial an additional angle was randomly added or subtracted to the standard

503   60° inducers. The initial difference was 2°. Following three correct responses, this difference

504   would decrease by a step size of 0.5°, or would increase by the same amount following a

505   single error. When an incorrect response was followed by three correct responses (i.e., a

506   reversal), the step size halved. If two incorrect responses were made in a row, the step size

507   would double. If the step size fell below 0.05°, it would be reset to 0.2°. Blocks consisted of

508   624 trials which took approximately 20 minutes including a forced break. Each observer

509   completed 16 blocks for a total of 9984 trials, which took a total of approximately five hours

510   duration spread over multiple days and testing sessions. To familiarize observers with the

511   task, they underwent two training blocks of 624 trials each with no noise. They then were

512   shown the stimulus with noise, and completed as many trials as they felt was required before

513   starting the experimental blocks.

514

515   **Support vector machine models.** Support vector machine (SVM) classifiers were trained

516   and tested in MATLAB. We generated (3) hypotheses by training SVM classifiers on images

517   of the *i*) inducers, *ii*) a triangle, or *iii*) a star. We trained the classifiers using a quadratic

518   kernel function and a least squares method of hyperplane separation. The training images

519   consisted of two exemplars ("narrow" and "wide") with no noise (**Supp. Fig. 1**). To generate

520   hypotheses in the form of classification images, we used each of the classifiers to perform

521   narrow/wide triangle judgements (trials = 9984), with an equilateral triangle; thus,

522   classification was exclusively influenced by the noise in the image.

19

523

524   **Data and statistical analysis.** The 9984 noise images for a participant were separated

525   according to perceptual report ("narrow" or "wide"). To collapse across inducer polarity, we

526   inverted the sign of noise on trials in which the cued inducers were white. We also collapsed

527   across upright and inverted cue conditions by spatially flipping the noise on inverted trials.

528   To calculate which spatial locations influenced perceptual reports, we used a standard

529   classification analysis in which each trial is classified according to the observer's response

530   with respect to the stimulus shown on that trial (Gold et al., 2000; Gold & Shubel, 2006;

531   Mareschal, Dakin, & Bex, 2006; Neri & Heeger, 2002). Each stimulus was either narrow or

532   wide (S_{narrow} or S_{wide}), and each response was either narrow or wide (R_{narrow} or R_{wide}), giving

533   four trial types: 1) $S_{narrow}R_{narrow}$, 2) $S_{wide}R_{narrow}$, 3) $S_{wide}R_{wide}$, 4) $S_{narrow}R_{wide}$. The classification

534   images were generated by averaging and combining these response types according to the

535   equation:

536   $$CI = (\overline{S_{\mathrm{narrow}}R_{\mathrm{narrow}}} + \overline{S_{\mathrm{wide}}R_{\mathrm{narrow}}}) - (\overline{S_{\mathrm{wide}}R_{\mathrm{wide}}} + \overline{S_{\mathrm{narrow}}R_{\mathrm{wide}}})$$

537

538   The resulting classification image shows the strength of correlation between each pixel's

539   location with the perceptual report made by the observer. Images are normalised to the

540   "attend upright black inducers" condition, such that black pixels indicate locations where

541   dark luminance noise was correlated with a narrow response, and light luminance noise was

542   correlated with a wide response. Conversely, white pixels indicate locations at which light

543   luminance noise was correlated with a narrow response, and dark luminance noise was

544   correlated with a wide response. The polarity and intensity of a given location thus provides

545   information regarding that location's contribution to perceptual decision making. To average

546   across emergent triangle edges, we further summed the image with itself two times after

547   rotating 120° and 240° using Matlab's "imrotate" function using bilinear interpolation. This

548   procedure results in a classification image that is invariant across edges such that analysis

549   of one edge summarises all three edges. Note that this is a conservative estimate of the

550   classification image and any spurious structure will only be diminished. To test for correlated

551   pixels along the illusory edge of the classification image, we extracted 18 pixels along the

552   bottom edge of the implied triangle, but within the bounds of the implied star tip (see bottom

553   right panel of **Fig. 2a**). To ensure that these pixels were not contaminated by averaging of

554 nearest-neighbour pixels during rotation, described above, we excluded the three pixels

555 closest to the inner corners of the star. We conducted a one-sample, two-tailed Bayesian

556 and Students' T-Test on these pixel values using JASP software (JASP Team, 2017).

557 Reported effect sizes are Cohen's d.

558

559 We performed the model comparisons in **Figure 2c** by first normalising the noise of the

560 mean classification image and each SVM prediction such that the sum of squared error of

561 each image equalled 1. We then subtracted the mean classification image from each

562 prediction, and found the sum of squared error of the resulting difference. Finally, we

563 normalised the difference scores to the model with the least error by subtracting from each

564 distribution the mean of the distribution with the lowest error. This process was repeated for

565 200 repetitions of each SVM prediction. The mixture modelling (**Fig. 3c**) was performed

566 similarly, but we further used Monte Carlo simulations to estimate the proportion of trials in

567 which a triangle was perceived. In this case, each set of 200 simulated experiments included

568 a proportion of triangle template trials, ranging from 0.33 (chance) to 1. We validated this

569 model fitting procedure by generating a simulated classification image with a known

570 generative template, or with proportional mixtures of templates, and then verified the model

571 fitting returned results that approximated the ground truth. The Monte Carlo simulations were

572 highly accurate for a range of simulated proportions, but slightly overestimated the

573 contribution of the triangle template when the ground truth contribution was close to 0.33,

574 and, conversely, slightly underestimated its contribution when the triangle was the only

575 contributor.

576

577 **Data availability**. The data that support the findings of this study are available from the

578 corresponding author upon request.

579

580 **ACKNOWLEDGEMENTS**

585   Cambridge and the National Health and Medical Research Council of Australia
586   (APP1091257).

587

AUTHOR CONTRIBUTIONS

589   Both authors designed the experiment and collected the data. WJH analysed the
590   experimental data, RR performed the SVM analyses, and both authors performed the model
591   comparisons. Both authors contributed equally to the writing of the manuscript.

592

593   We declare we have no competing interests.

594

REFERENCES

Abbey, C. K., Eckstein, M. P., & Bochud, F. O. (1999). Estimation of human-observer templates in two-alternative forced-choice experiments. In E. A. Krupinski (Ed.) (Vol. 3663, pp. 284–295). International Society for Optics and Photonics. https://doi.org/10.1117/12.349653

Abrams, J., Barbot, A., & Carrasco, M. (2010). Voluntary attention increases perceived spatial frequency. *Attention, Perception & Psychophysics*, *72*(6), 1510–1521. https://doi.org/10.3758/APP.72.6.1510

Ahumada, A. J. (1996). Perceptual Classification Images from Vernier Acuity Masked by Noise. *Perception*, *25*(1 suppl), 2–2. https://doi.org/10.1068/v96l0501

Ahumada, A. J. . J., Beard, B. L., & Ellis, S. R. (1997). Response Classification Images in Vernier Acuity.

Ahumada, A., & Lovell, J. (1971). Stimulus Features in Signal Detection. *The Journal of the Acoustical Society of America*, *49*(6B), 1751–1756. https://doi.org/10.1121/1.1912577

Anton-Erxleben, K., Henrich, C., & Treue, S. (2007). Attention changes perceived size of moving visual patterns. *Journal of Vision*, *7*(11), 5. https://doi.org/10.1167/7.11.5

Barbot, A., Liu, S., Kimchi, R., & Carrasco, M. (2018). Attention enhances apparent perceptual organization. *Psychonomic Bulletin and Review*, *25*(5), 1824–1832. https://doi.org/10.3758/s13423-017-1365-x

Beard, B. L., & Ahumada, Jr., A. J. (1998). A Technique to extract relevant image features for visual tasks. In B. E. Rogowitz & T. N. Pappas (Eds.), *Human Vision and Electronic Imaging III* (Vol. 3299, pp. 79–85). International Society for Optics and Photonics. https://doi.org/10.1117/12.320099

619   Brainard, D. H. (1997). The Psychophysics Toolbox. *Spatial Vision*, *10*(4), 433–436.

620   Carrasco, M. (2011). Visual attention: the past 25 years. *Vision Research*, *51*(13), 1484–

621   1525. https://doi.org/10.1016/j.visres.2011.04.012

622   Carrasco, M., Ling, S., & Read, S. (2004). Attention alters appearance. *Nature*

623   *Neuroscience*, *7*(3), 308–313. https://doi.org/10.1038/nn1194

624   Cornelissen, F. W., Peters, E. M., & Palmer, J. (2002). The Eyelink Toolbox: eye tracking

625   with MATLAB and the Psychophysics Toolbox. *Behavior Research Methods,*

626   *Instruments & Computers*, *34*(4), 613–617.

627   Davis, G., & Driver, J. (1994). Parallel detection of Kanizsa subjective figures in the human

628   visual system. *Nature, 371*(6500), 791–793. https://doi.org/10.1038/371791a0

629   Driver, J., & Baylis, G. C. (1996). Edge-assignment and figure-ground segmentation in short-

630   term   visual   matching.   *Cognitive   Psychology*,   *31*(3),   248–306.

631   https://doi.org/10.1006/cogp.1996.0018

632   Gobell, J., & Carrasco, M. (2005). Attention alters the appearance of spatial frequency and

633   gap size. *Psychological Science*, *16*(8), 644–651. https://doi.org/10.1111/j.1467-

634   9280.2005.01588.x

635   Gold, J. M., Murray, R. F., Bennett, P. J., & Sekuler, A. B. (2000). Deriving behavioural

636   receptive fields for visually completed contours. *Current Biology*, *10*(11), 663–666.

637   https://doi.org/10.1016/S0960-9822(00)00523-6

638   Gold, J. M., & Shubel, E. (2006). The spatiotemporal properties of visual completion

639   measured   by   response   classification.   *Journal   of   Vision*,   *6*(4),   5–5.

640   https://doi.org/10.1167/6.4.5

641   Harrison, W. J., Ayeni, A. J., & Bex, P. J. (2019). Attentional selection and illusory surface

642   appearance. *Scientific Reports*.

24

643   Houtkamp, R., Spekreijse, H., & Roelfsema, P. R. (2003). A gradual spread of attention
644   during mental curve tracing. *Perception and Psychophysics*, *65*(7), 1136–1144.

645   Kanizsa, G. (1976). Subjective contours. *Scientific American*, *234*(4), 48–52.

646   Liu, T., Abrams, J., & Carrasco, M. (2009). Voluntary attention enhances contrast
647   appearance. *Psychological Science*, *20*(3), 354–362. https://doi.org/10.1111/j.1467-
648   9280.2009.02300.x

649   Mareschal, I., Dakin, S. C., & Bex, P. J. (2006). Dynamic properties of orientation
650   discrimination assessed by using classification images. *Proceedings of the National*
651   *Academy of Sciences of the United States of America*, *103*(13), 5131–5136.
652   https://doi.org/10.1073/pnas.0507259103

653   Mattingley, J. B., Davis, G., & Driver, J. (1997). Preattentive filling-in of visual surfaces in
654   parietal extinction. *Science*, *275*(5300), 671–674.

655   McMains, S., & Kastner, S. (2011). Interactions of Top-Down and Bottom-Up Mechanisms
656   in Human Visual Cortex. *Journal of Neuroscience*, *31*(2), 587–597.
657   https://doi.org/10.1523/JNEUROSCI.3766-10.2011

658   Mihalas, S., Dong, Y., von der Heydt, R., & Niebur, E. (2011). Mechanisms of perceptual
659   organization provide auto-zoom and auto-localization for attention to objects.
660   *Proceedings of the National Academy of Sciences of the United States of America*,
661   *108*(18), 7583–7588. https://doi.org/10.1073/pnas.1014655108

662   Murray, M. M., Wylie, G. R., Higgins, B. a, Javitt, D. C., Schroeder, C. E., & Foxe, J. J.
663   (2002). The spatiotemporal dynamics of illusory contour processing: combined high-
664   density electrical mapping, source analysis, and functional magnetic resonance
665   imaging. *The Journal of Neuroscience : The Official Journal of the Society for*
666   *Neuroscience*, *22*(12), 5055–5073. https://doi.org/22/12/5055 [pii]

25

667   Necker, L. A. (1832). LXI. Observations on some remarkable optical phænomena seen in

668   Switzerland; and on an optical phænomenon which occurs on viewing a figure of a

669   crystal or geometrical solid. *The London, Edinburgh, and Dublin Philosophical*

670   *Magazine and Journal of Science*, *1*(5), 329–337.

671   https://doi.org/10.1080/14786443208647909

672   Neri, P., & Heeger, D. J. (2002). Spatiotemporal mechanisms for detecting and identifying

673   image features in human vision. *Nature Neuroscience*, *5*(8), 812–816.

674   https://doi.org/10.1038/nn886

675   Pelli, D. G. (1997). The VideoToolbox software for visual psychophysics: Transforming

676   numbers into movies. *Spatial Vision*, *10*(4), 437–442.

677   Poort, J., Raudies, F., Wannig, A., Lamme, V. A. F., Neumann, H., & Roelfsema, P. R.

678   (2012). The role of attention in figure-ground segregation in areas V1 and V4 of the

679   visual cortex. *Neuron*, *75*(1), 143–156. https://doi.org/10.1016/j.neuron.2012.04.032

680   Posner, M. I. (1980). Orienting of attention. *Quarterly Journal of Experimental Psychology*,

681   *32*(1), 3–25.

682   Posner, M. I. (2014). Orienting of attention: Then and now. *The Quarterly Journal of*

683   *Experimental Psychology*, 1–12. https://doi.org/10.1080/17470218.2014.937446

684   Qiu, F. T., Sugihara, T., & von der Heydt, R. (2007). Figure-ground mechanisms provide

685   structure for selective attention. *Nature Neuroscience*, *10*(11), 1492–1499.

686   https://doi.org/10.1038/nn1989

687   Ringach, D. L., & Shapley, R. (1996). Spatial and temporal properties of illusory contours

688   and amodal boundary completion. *Vision Research*, *36*(19), 3037–3050.

689   Rubin, E. (1915). *Synsoplevede Figurer. Studier i psykologisk Analyse /Visuell*

690   *wahrgenommene Figuren. Studien in psychologischer Analyse [Visually perceived*

26

691   *figures: Studies in psychological analysis]*. Copenhagen, Denmark: Gyldendalske

692   Boghandel.

693 Shapley, R., Rubin, N., & Ringach, D. (2004). Visual segmentation and illusory contours. In

694   L. M. Chalupa & J. S. Werner (Eds.), *The Visual Neurosciences* (pp. 1119–1128).

695   MIT Press. Retrieved from http://www.cns.nyu.edu/ nava/MyPubs/Shapley-Rubin-

696   Ringach_VisSeg_MITpress2004.pdf

697 Stanley, D. A., & Rubin, N. (2003). fMRI activation in response to illusory contours and

698   salient regions in the human Lateral Occipital Complex. *Neuron, 37*(2), 323–331.

699   https://doi.org/10.1016/S0896-6273(02)01148-0

700 Stormer, V. S., McDonald, J. J., & Hillyard, S. A. (2009). Cross-modal cueing of attention

701   alters appearance and early cortical processing of visual stimuli. *Proceedings of the*

702   *National Academy of Sciences, 106*(52), 22456–22461.

703   https://doi.org/10.1073/pnas.0907573106

704 Tse, P. U. (2005). Voluntary attention modulates the brightness of overlapping transparent

705   surfaces. *Vision Research, 45*(9), 1095–1098.

706   https://doi.org/10.1016/j.visres.2004.11.001

707 Turatto, M., Vescovi, M., & Valsecchi, M. (2007). Attention makes moving objects be

708   perceived to move faster. *Vision Research, 47*(2), 166–178.

709   https://doi.org/10.1016/j.visres.2006.10.002

710 van Lier, R., Vergeer, M., & Anstis, S. (2009). Filling-in afterimage colors between the lines.

711   *Current Biology, 19*(8), R323–4. https://doi.org/10.1016/j.cub.2009.03.010

712 von der Heydt, R, Peterhans, E., & Baumgartner, G. (1984). Illusory contours and cortical

713   neuron responses. *Science, 224*(4654), 1260–1262.

714   https://doi.org/10.1126/science.6539501

715   von der Heydt, Rüdiger, Macuda, T., & Qiu, F. T. (2005). Border-ownership-dependent tilt

716   aftereffect. *Journal of the Optical Society of America A, 22*(10), 2222.

717   https://doi.org/10.1364/JOSAA.22.002222

718   Wagemans, J., Elder, J. H., Kubovy, M., Palmer, S. E., Peterson, M. A., Singh, M., & von

719   der Heydt, R. (2012). A century of Gestalt psychology in visual perception: I.

720   Perceptual grouping and figure-ground organization. *Psychological Bulletin, 138*(6),

721   1172–1217. https://doi.org/10.1037/a0029333

722   Wannig, A., Stanisor, L., & Roelfsema, P. R. (2011). Automatic spread of attentional

723   response modulation along Gestalt criteria in primary visual cortex. *Nature

724   Neuroscience, 14*(10), 1243–1244. https://doi.org/10.1038/nn.2910

725   Zhou, H., Friedman, H. S., & von der Heydt, R. (2000). Coding of border ownership in

726   monkey   visual   cortex.   *Journal   of   Neuroscience,   20*(17),   6594.

727   https://doi.org/10.1523/JNEUROSCI.2797-12.2013

728

729

730 **SUPPLEMENTARY FIGURES**
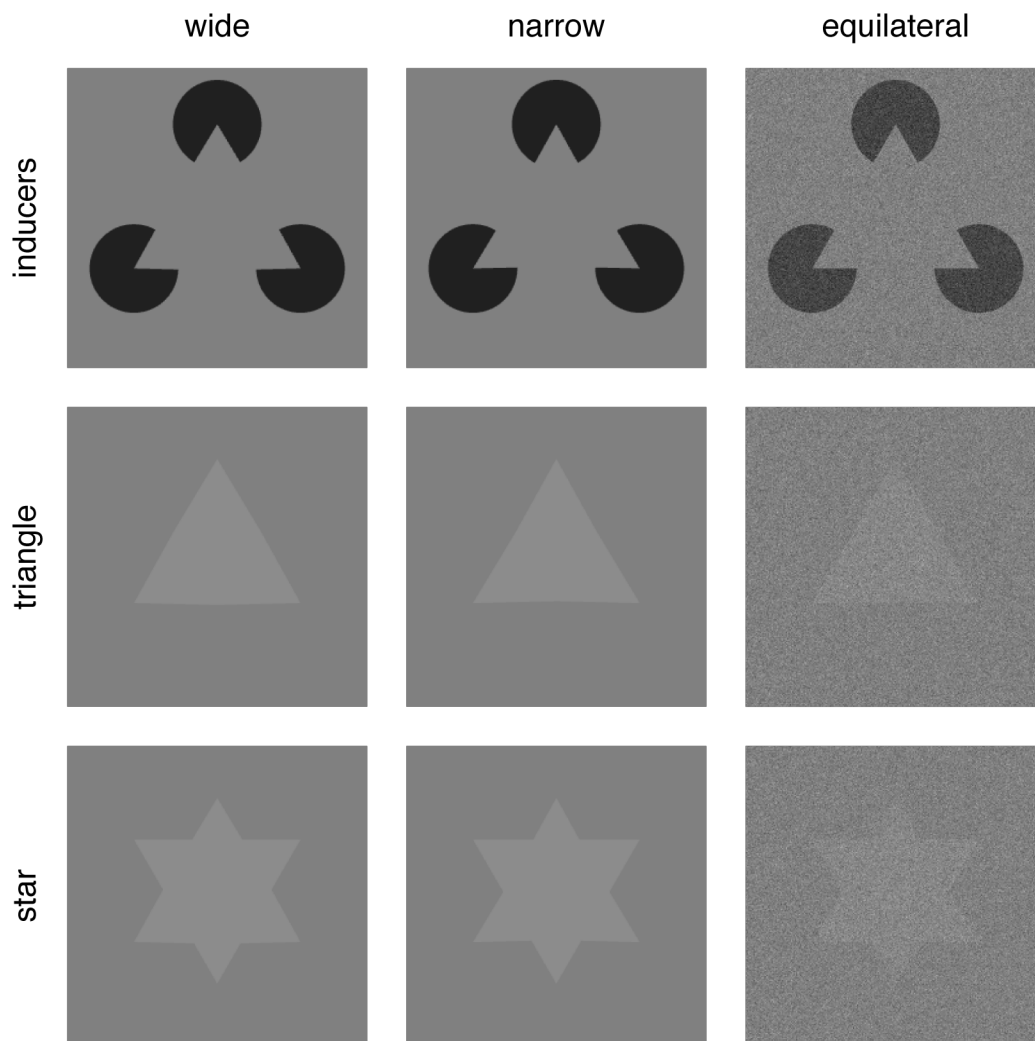
731

732 **Supplementary Figure 1**. Support vector machine (SVM) images. From left to right, the first two columns

733 show examples of wide and narrow exemplar images used to train the SVM in the inducers, triangle, and star

734 protocols. The column on the right shows examples of the test image for each protocol.

735
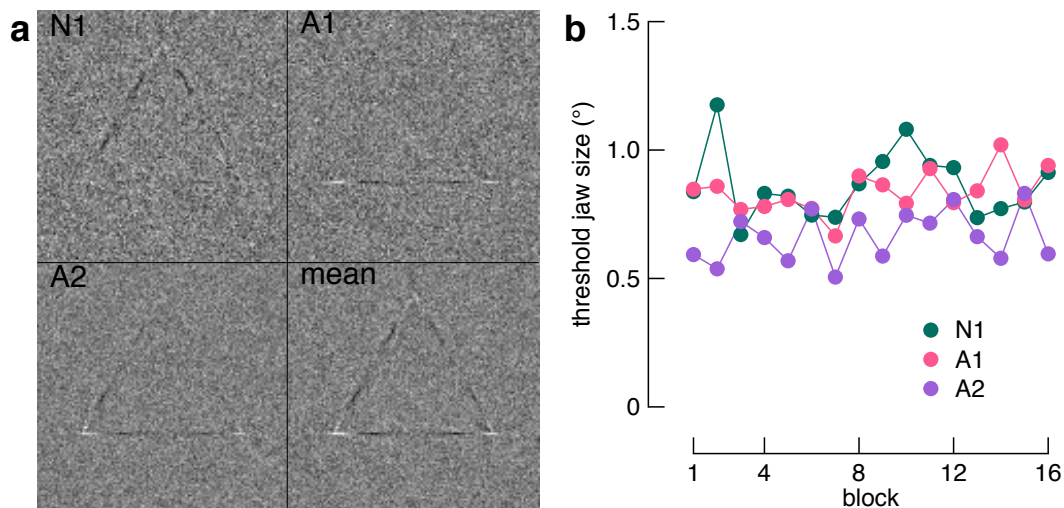
Supplementary Figure 2. Raw classification images and psychophysical performance. a) Classification images without averaging of edges via rotation. Note that the individual images show varying degrees of a complete triangle. One explanation for this is that observers perceived a partial shape, e.g., a single or pair of unconnected lines between the cued inducers. Given the strength of the Kanizsa illusion in producing the percept of a triangle, rather than a partial shape, a more likely explanation is that observers perceived a triangle, but only used part of this triangle to perform the task. b) Threshold performance across blocks shown separately for each observer. Thresholds were the midpoint of a cumulative Gaussian fit to accuracy data for each session.

747
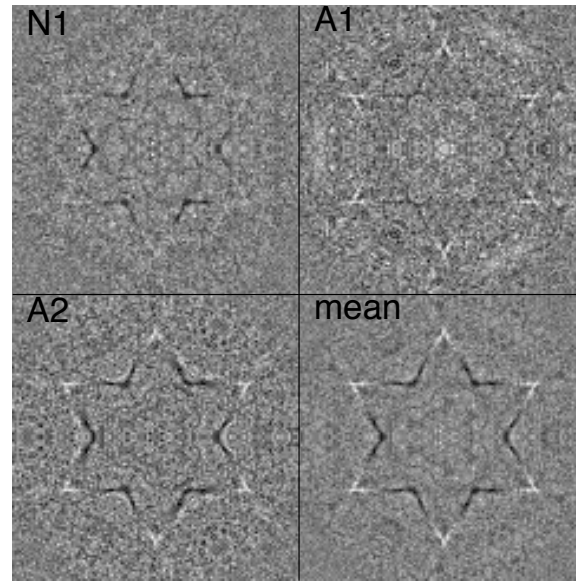
748 **Supplementary Figure 3**. Individual classification images revealing a potential influence of non-cued

749 structure. These images were created by summing each classification image with a flipped version of itself.

750 Note that the emergent structure aligns to the geometry of the star implied by our Kanizsa figure (**Fig. 1a**).